Modulation of Majorana-Induced Current Cross-Correlations by Quantum Dots

Björn Zocher[1,2] and Bernd Rosenow[1]

[1]Institut für Theoretische Physik, Universität Leipzig, D-04103 Leipzig, Germany
[2]Max Planck Institut für Mathematik in den Naturwissenschaften, D-04103 Leipzig, Germany

(Received 23 August 2012; published 18 July 2013)

We study charge transport through a topological superconductor with a pair of Majorana end states coupled to leads via quantum dots with resonant levels. The nonlocality of the Majorana bound states opens the possibility of crossed Andreev reflection with nonlocal shot noise due to the injection of an electron into one end of the superconductor followed by the emission of a hole at the other end. In the space of energies of the two resonant quantum dot levels, we find a four peaked cloverlike pattern for the strength of noise due to crossed Andreev reflection, distinct from the single ellipsoidal peak found in the absence of Majorana bound states.

DOI: 10.1103/PhysRevLett.111.036802 PACS numbers: 73.21.−b, 03.75.Lm, 74.45.+c, 74.78.Na

Majorana bound states (MBSs) are zero-energy fermionic states which are their own antiparticles. Since quasiparticles (QPs) in superconductors (SCs) are always superpositions of electron and hole components, the Majorana criterion can be realized in a peculiar way: a zero-energy QP in a SC has equal contributions from electrons and holes, and hence, an exchange of electron and hole components leaves the QP invariant. There is currently much interest in the physics of MBSs [1–8], since one pair of MBSs nonlocally encodes a qubit, which is the building block for fault-tolerant topological quantum computing architectures [9,10].

There is a variety of candidate systems for realizing Majorana fermions. Early proposals considered time-reversal symmetry broken p-wave SCs with the candidate Sr_2RuO_4 [11]. Recently, the SC proximity effect has been suggested as a way to effectively induce p-wave pairing in topological insulators [12] and semiconductors with strong Rashba spin-orbit coupling [13–16]. Recent experiments reported evidence of MBSs in semiconductor-superconductor heterostructures [1–5]. A possible probe for the nonlocal nature of MBSs is crossed Andreev reflection (CAR), the conversion of an incoming electron into an outgoing hole in a different lead [17–22], in contrast to local Andreev reflection (LAR), where electron and hole reside in the same lead. It has been shown theoretically that at sufficiently low voltages and small level width, CAR by the pair of MBSs dominates transport [23–29]. For voltages larger than the MBS energy splitting ϵ_M, however, resonant tunneling of electrons and holes gives rise to negative cross-correlations, and the total crossed noise vanishes.

In this Letter, we focus on the physics of coupling a pair of MBSs at the ends of a wire to leads via resonant quantum dot (QD) levels in the Coulomb blockade regime, see Fig. 1. As demonstrated in recent experiments [30–32], the QDs suppress LAR. Because of the finite wire length, the MBSs are tunnel coupled to each other and have an energy splitting $\epsilon_M \sim \Delta \exp(-L/\xi_{SM})$, where ξ_{SM} is the coherence length in the semiconductor. Whenever one of the dot levels is aligned with the chemical potential of the superconductor, a MBS forms on that dot at exactly zero energy [33], even for ϵ_M finite. Hence, the MBSs at the ends of the wire are effectively uncoupled, and no CAR can be observed. When tuning the dot levels away from the chemical potential of the superconductor, the coupling between the MBSs is restored. In addition, negative cross-correlations due to resonant tunneling are suppressed, and CAR becomes visible in positive current cross-correlations. Thus, the crossed current correlator provides a clear signature of nonlocal transport through a pair of MBSs in the form of a four-leaf clover feature as a function of ϵ_L and ϵ_R, observable best in the regime of level broadenings Γ_L, $\Gamma_R \gg \epsilon_M$. These findings are in excellent agreement with results for a microscopic model of a spinless p-wave SC [34], they persist in a more realistic model with several transverse channels, and are robust against addition of disorder. We stress that the mechanism leading to cross-correlations $\propto (e^2/h)\epsilon_M^2/\Gamma$ is a finite energy splitting ϵ_M and not phase coherent electron

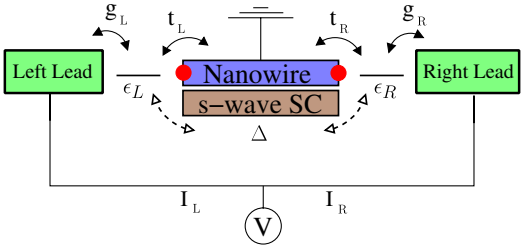

FIG. 1 (color online). Schematic setup for a system with a pair of Majorana bound states (red dots) coupled to quantum dots which themselves are coupled to lead electrodes. The leads are biased with the positive chemical potential eV. Crossed Andreev reflection can be detected by correlating the currents I_L and I_R that flow into the SC nanowire via MBSs. The nearby s-wave SC also induces a proximity pairing Δ between the dots.

teleportation as discussed in Ref. [35]. We note that the crossed noise in a similar system was recently studied in Ref. [36] within the diagonalized master equation approach. There, it was found that the crossed noise stays finite in the limit $\epsilon_M \to 0$, different from our finding that it is proportional to ϵ_M^2 and thus vanishes. For a discussion of reasons for this disagreement, see Ref. [37].

Model system.—We consider the Hamiltonians

$$H_D = \sum_{i=L,R} (\epsilon_i d_i^\dagger d_i + g_i d_i^\dagger \psi_i + g_i^* \psi_i^\dagger d_i), \tag{1a}$$

$$H_M = \epsilon_M i\gamma_L\gamma_R + \sum_{i=L,R} (t_i^* d_i^\dagger \gamma_i + t_i \gamma_i d_i), \tag{1b}$$

$$H_S = \Delta(d_L^\dagger d_R^\dagger + d_R d_L). \tag{1c}$$

Here, H_D describes two QDs coupled to leads, where d_i annihilates an electron with energy ϵ_i on dot i, ψ_i annihilates a lead electron, and g_i is the lead-dot coupling strength. The lead electrons are characterized by their density of states ρ_i, which is assumed to be energy independent and have a chemical potential eV. We consider the regime where the QD single particle level spacing $\delta\epsilon$ satisfies $\delta\epsilon > eV > k_B T$. We assume that the spin degeneracy is lifted by an external magnetic field and that the QD ground state has an even number of electrons. Then, Kondo physics is absent, and in the Coulomb blockade regime, inclusion of only a single dot level in H_D is justified. H_M describes two MBSs with an energy splitting ϵ_M coupled to the dots. The MBSs are described by Hermitian operators $\gamma_i = \gamma_i^\dagger$, which have anticommutators $\{\gamma_i, \gamma_j\} = 2\delta_{i,j}$ and are coupled to QD i with amplitude t_i. The chemical potential of the SC wire hosting the MBS is zero. H_S describes an additional proximity-induced pairing between the dots with an amplitude $\Delta \sim \gamma_S \sin(k_F L) \times \exp(-L/\xi_{SC})/(k_F L)$ [21], where γ_S is the normal-state QD level broadening due to the coupling between SC and QD, k_F is the Fermi momentum, L is the length, and ξ_{SC} is the coherence length of the SC. We have in mind that this term may mainly be due to a coupling between the dots and the s-wave SC in a hybrid structure.

We diagonalize the Hamiltonian for MBSs and QDs without lead coupling by solving the corresponding Bogoliubov–de Gennes equation $h\Psi = \epsilon(\mathbb{I}_D + (1/2)\mathbb{I}_M)\Psi$ with

$$h = \begin{pmatrix} 0 & i\epsilon_M & t_L & 0 & -t_L^* & 0 \\ -i\epsilon_M & 0 & 0 & t_R & 0 & -t_R^* \\ t_L^* & 0 & \epsilon_L & 0 & 0 & \Delta \\ 0 & t_R^* & 0 & \epsilon_R & -\Delta & 0 \\ -t_L & 0 & 0 & -\Delta & -\epsilon_L & 0 \\ 0 & -t_R & \Delta & 0 & 0 & -\epsilon_R \end{pmatrix} \tag{2}$$

in the basis $\{\gamma_L, \gamma_R, d_L^\dagger, d_R^\dagger, d_L, d_R\}$. Here, $\mathbb{I}_D$ ($\mathbb{I}_M$) denote the identity matrix in the dot (Majorana) space. In the case $\Delta = 0$, the QP energy spectrum has levels at $2\epsilon_M$, ϵ_R, and ϵ_L, with avoided crossings where these levels intersect each other. If one of the dot levels resides at the chemical potential of the SC, e.g., $\epsilon_L = 0$, we always find one zero-energy state described by the Majorana operators

$$\gamma_1 = \frac{t_L^* d_L^\dagger + t_L d_L}{|t_L|}, \tag{3}$$

$$\gamma_2 = \frac{2|t_L|(t_R^* d_R^\dagger + t_R d_R - \epsilon_R\gamma_R) + i(\epsilon_M\epsilon_R/|t_L|)(t_L^* d_L^\dagger - t_L d_L)}{\sqrt{\epsilon_R^2\epsilon_M^2 + 2|t_L|^2(\epsilon_R^2 + 2|t_R|^2)}}. \tag{4}$$

Here, γ_1 is localized on the resonant dot, while γ_2 is partially delocalized, and the weight of γ_2 on the resonant dot is determined by the energy ϵ_R of the nonresonant level. In particular for $\epsilon_L = \epsilon_R = 0$, we find $\gamma_2 = (t_R^* d_R^\dagger + t_R d_R)/|t_R|$ [38]. These induced zero-energy states are topologically not protected and acquire a finite energy $\epsilon_L\epsilon_R\epsilon_M/2|t_L t_R|$ for $\epsilon_L\epsilon_R \neq 0$.

To compute the zero-frequency noise through the above-noted normal-state–SC–normal-state system, we use a scattering matrix approach which also allows for Andreev reflection processes [39]. This yields the current and the noise correlators

$$I_i = \frac{e}{h}\int d\epsilon \sum_\alpha \mathrm{sgn}(\alpha) \sum_{k;\gamma} A^{(i\alpha)}_{k,k;\gamma,\gamma} n_{k,\gamma}, \tag{5}$$

$$S_{ij} = \frac{2e^2}{h}\int d\epsilon \sum_{\alpha,\beta} \mathrm{sgn}(\alpha\beta) \sum_{k,l;\gamma,\delta} A^{(i\alpha)}_{k,l;\gamma,\delta} A^{(j\beta)}_{l,k;\delta,\gamma} n_{k,\gamma}(1 - n_{l,\delta}), \tag{6}$$

where greek indices denote electron (e) and hole (h) channels, $\mathrm{sgn}(e) = +1$ and $\mathrm{sgn}(h) = -1$, roman indices denote the left (L) and right (R) lead, and

$$A^{(i\alpha)}_{k,l;\beta,\gamma} = \delta_{ik}\delta_{il}\delta_{\alpha\beta}\delta_{\alpha\gamma} - s^{\alpha\beta *}_{i,k} s^{\alpha\gamma}_{i,l}. \tag{7}$$

The reservoir distribution functions $n_{k,\gamma}$ are Fermi functions with different chemical potentials for the electron and hole bands $n_{k,\gamma} = 1/(1 + \exp\{\beta[\epsilon - \mathrm{sgn}(\gamma)eV_k]\})$. For the setup Fig. 1, $V_L = V_R \equiv V$. The coefficients $s^{\alpha,\beta}_{i,j}$ are the elements of the S matrix

$$S(\epsilon) = 1 - 2\pi i W^\dagger [\epsilon\mathbb{I}_D + (\epsilon/2)\mathbb{I}_M - h + i\pi W W^\dagger]^{-1} W, \tag{8}$$

where W describes the coupling between the states of the system without leads and the scattering states in the leads, and $[\epsilon(\mathbb{I}_D + 1/2\mathbb{I}_M) - h + i\pi W W^\dagger]^{-1}$ is the retarded electron Green function for the closed system with self-energy $i\pi W W^\dagger$. The coupling matrix W in the lead basis $\{\psi_L^\dagger, \psi_R^\dagger, \psi_L, \psi_R\}$ is given by

$$W_{i_l\alpha_{i_l}, i_d\alpha_{i_d}} = \mathrm{sgn}(\alpha_{i_d}) g_{i_l} \sqrt{\rho_{i_l}} \delta_{i_l,i_d} \delta_{\alpha_{i_l},\alpha_{i_d}}, \tag{9}$$

where α_{i_d} (α_{i_l}) denotes the particle species of QD i_d (lead i_l). The coupling strengths g_i give rise to the level

broadening $\Gamma_i = 2\pi\rho_i|g_i|^2$ in the dots. In the following, we consider the case $\Gamma_L = \Gamma_R \equiv \Gamma$, $t_L = t_R \equiv t$, and take the limit of zero temperature.

Weak dot-lead coupling.—We begin our analysis in the regime $\Delta = 0$ and $\Gamma < t < \epsilon_M$. In Fig. 2, both differential conductance and crossed current correlator S_{LR} are displayed as a function of bias voltage for several characteristic points in the ϵ_L-ϵ_R plane. The differential conductance is peaked at the eigenenergies of Eq. (2). The peak width is determined by the broadening Γ. If one of the dot levels resides at the chemical potential of the SC, we always find a zero bias peak with height $4(e^2/h)/[1 + \epsilon_M^2(\epsilon_R^2 + \Gamma^2/4)/4|t_L t_R|^2]$ in the differential conductance, due to the existence of the induced Majorana states Eq. (4). Since the existence of a zero-energy MBS implies a strongly reduced coupling between the left and right side of the wire, we find that these resonances yield only a small contribution to the crossed noise despite their large conductance.

In contrast, we do not find a zero-bias conductance peak if both dots are nonresonant. In this regime, there is a striking difference between symmetric ($\epsilon_L = \epsilon_R$) and antisymmetric ($\epsilon_L = -\epsilon_R$) positions of the dot levels. In both cases, we find contributions to the conductance and S_{LR} due to the hybridization between the dots and the MBS. However, in the antisymmetric case, both the conductance and S_{LR} are much larger than in the symmetric case, and additional resonances at the QD energies contribute to crossed noise. This is due to the fact that Cooper pairs have zero energy, which leads to a suppression of transmission through two resonant levels which have both the same energy in the symmetric case but allows passage through QDs with opposite level energies in the antisymmetric case.

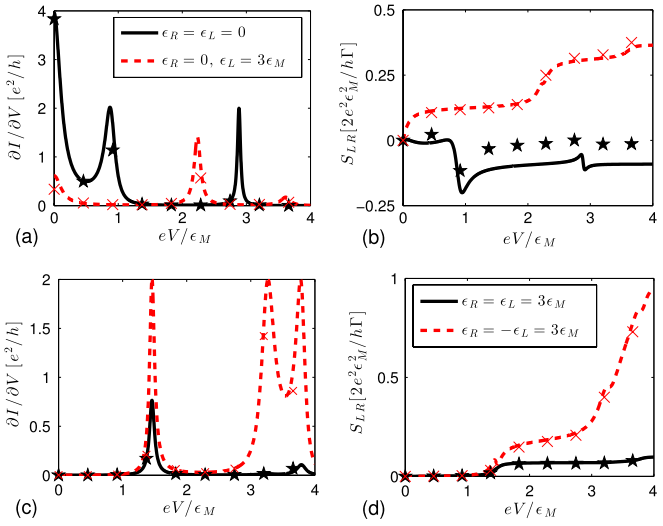

FIG. 2 (color online). Current cross-correlator S_{LR} in the weak dot-lead coupling regime with $\Gamma = \epsilon_M/4$, $t = 0.8\epsilon_M$, and $\Delta = 0$. The lines for panel (b) are defined in (a), those for panel (c) in (d). The markers denote the results for the spinless SC model with $\epsilon_M = 0.01$ meV and $\Gamma = 0.002$ meV.

These findings agree very well with the results for the microscopic model of a spinless p-wave SC defined in Eq. (10), see Fig. 2. The only small deviation in S_{LR} can be seen if both dots are resonant, where the effective model has a small negative S_{LR} for large bias voltage, while it approaches zero for the microscopic model. This deviation has its origin in the presence of an additional transport channel due to a proximity coupling Δ in the microscopic model, which in principle could be described by the Hamiltonian H_S in Eq. (1c), but which is not included in the effective model $H = H_M + H_D$ considered here.

Strong dot-lead coupling.—We consider the case $t < \epsilon_M \ll \Gamma$ and begin with the situation $\Delta = 0$. In Fig. 3(a), the correlator S_{LR} for $\epsilon_M \ll eV = \Gamma/2$ in the ϵ_L-ϵ_R plane is shown. It is characterized by a four-leaf clover feature with a suppression of crossed noise along lines with either $\epsilon_L = 0$ or $\epsilon_R = 0$ and peaks at $|\epsilon_L| = |\epsilon_R| \approx \Gamma/2$. While the peak height scales with ϵ_M^2/Γ, the width of these peaks is larger than the Majorana energy splitting due to the large value of Γ. As before, the suppression of the noise along $\epsilon_L = 0$ and $\epsilon_R = 0$ is mediated by the formation of zero-energy Majorana modes by virtue of the dot-MBS coupling, which corresponds to the case of uncoupled MBSs.

The emergence of an approximate symmetry between symmetric and antisymmetric positions of the dot levels (absent in the case $\Gamma < t$) can be understood as follows. For large Γ, the dots are strongly coupled to the leads and effectively become part of them. Hence, there are no separate resonances at the positions of the QD levels anymore, and only a single resonance due to the MBS in the wire survives. Since $t \ll \Gamma$, the broadening of this resonance is much smaller than Γ. As the QD levels can neither resolve this small broadening of the resonance nor resolve the location of the resonance, the distinction between symmetric and antisymmetric QD levels becomes blurred, and the approximate symmetry arises. The Majorana zero-energy state residing on one of the dots for $\epsilon_L = 0$ or $\epsilon_R = 0$, however, does not change its character due to the presence of a large broadening Γ, and the noise stays

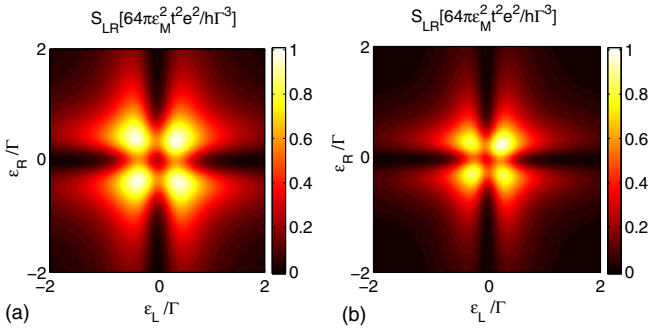

FIG. 3 (color online). Current cross-correlator S_{LR} for strong dot-lead coupling. (a) Effective model with $eV = \Gamma/2$, $t = \Gamma/20$, $\epsilon_M = \Gamma/10$, and $\Delta = 0$. (b) Spinless SC with $\epsilon_M = 0.01$ meV and $\Gamma = 0.06$ meV. For both (a) and (b), the pattern changes little for larger eV.

low in this case, giving rise to the cloverlike pattern in Fig. 3(a).

In Fig. 3(b), we complement these findings with results for the microscopic model Eq. (10), for which a similar four-leaf clover structure emerges. However, similar to the weak dot-lead coupling regime, there are small deviations with respect to the effective model near $\epsilon_L = \epsilon_R = 0$, mediated by the SC proximity effect.

For finite temperatures T, the amplitude of the symmetrically arranged peaks in the cloverlike pattern decreases and becomes negative while the antisymmetrically arranged peaks remain unchanged. Hence, for $k_B T > \Gamma$, the pattern from Fig. 3(a) is modulated in such a way that the peaks for symmetric dot levels become negative of the same height [37].

To gain insight into the effect of an additional proximity term H_S, we first discuss the situation without MBSs, $H = H_D + H_S$. In Fig. 4(a), the crossed current correlator for the SC proximity case is shown. Here, S_{LR} has a single peak of height $\propto \Delta^2/\Gamma$ near $\epsilon_L = \epsilon_R = 0$, with width Γ along the direction $\epsilon_L = \epsilon_R$, and width eV along the direction $\epsilon_L = -\epsilon_R$. In contrast to the MBS case, there is no additional structure in this peak.

In Fig. 4(b), we consider the combined Hamiltonian $H = H_M + H_D + H_S$. We find a four-leaf clover feature similar to that in the Majorana only case, with the center of this feature now having a peak due to the proximity term in H_S. From this, we conclude that the contributions from the proximity effect and the MBS-mediated CAR approximately add up. The relative peak heights in the crossed current correlator reflect the ratio of Δ^2 and ϵ_M^2.

Microscopic model.—We complement our calculations by the analysis of a microscopic model for a spinless p-wave SC with Hamiltonian [34],

$$H_K = -\sum_{j=1}^{N-1}(t_K c_{j+1}^\dagger c_j + \Delta_K c_j c_{j+1} + \text{H.c.}) - \mu_K \sum_{j=1}^{N} c_j^\dagger c_j, \tag{10}$$

where the c_j annihilate a spinless fermion on site j with nearest neighbor hopping t_K and nearest neighbor pairing amplitude Δ_K. This model describes the low-energy physics of a nanowire in the topologically nontrivial phase. In the numerical analysis, we use the parameters $L = 1000$ nm for the wire length, $N = 200$ sites, $t_K = 20$ meV, $\Delta_K = 0.8$ meV, and $\mu_K = 39.4$ meV, similar to the parameters used in Ref. [40]. These parameter values yield the SC gap $\Delta_{\text{SC}} = 0.3$ meV and the Majorana energy splitting $\epsilon_M = 0.01$ meV. For the coupling of the operators c_1 and c_N to the dots, we use $t_{D,K} = 0.025$ meV. The results for this model agree very well with those for the effective model Eq. (1c), see Figs. 2 and 3. By introducing a finite wire width, we generalized this model to multichannel p-wave SCs where the cloverlike pattern remains for transverse channel number $N_\perp < 4\pi(v_F \Delta_{\text{SC}}/\sqrt{\xi} T_{\text{SD}} \Gamma)$ [37]. Here, v_F is the Fermi velocity and T_{SD} is the wire-dot coupling strength. For the parameters used in Fig. 3(b), this yields the condition $N_\perp \leq 7$. Furthermore, we find that the cloverlike pattern is robust against disorder of strength $\lesssim \Delta_{\text{SC}}$ [37].

The Majorana energy splitting ϵ_M is oscillating as a function of the chemical potential with periodicity $2\pi v_F/L$ when neglecting the long-range Coulomb interaction [41]. Since the minima of $\epsilon_M(\mu)$ are zero, the Majorana-induced current cross-correlations vanish. Thus, the chemical potential can be used to switch the crossed noise between the cloverlike pattern (Fig. 3) and the ellipsoidal pattern (Fig. 4). In the experiment, this variation of the chemical potential can be realized by applying a global gate voltage to the topologically nontrivial sector of the nanowire.

Conclusion.—The nonlocality of a pair of Majorana bound states can be probed by crossed Andreev reflection, whose observation is facilitated when suppressing local Andreev reflection with the help of two resonant QDs. In the case of a weak coupling between QDs and leads, we find a set of discrete transmission resonances. When at least one of the QD levels is tuned to the chemical potential of the superconductor, a zero-energy Majorana state forms in the respective QD, which contributes only weakly to crossed Andreev reflection. This feature survives in the limit of strong dot-lead coupling, giving rise to a cloverlike modulation of crossed shot noise as a function of QD energies, which is different from the single peak found without Majorana states.

We acknowledge helpful discussions with A. Das, M. Heiblum, and M. Horsdal, as well as financial support from the Federal Ministry of Education and Research (BMBF).

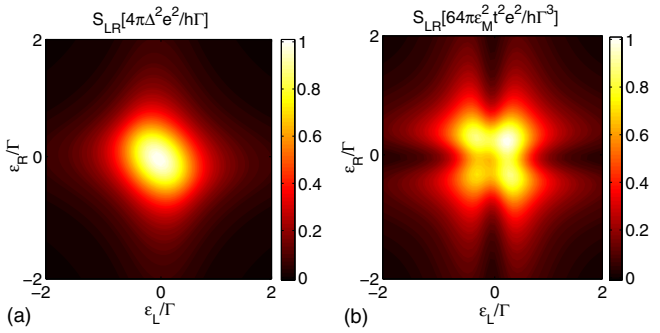

FIG. 4 (color online). Current cross-correlator S_{LR} for $eV = \Gamma/2$. The dots are coupled (a) via the SC proximity effect with $\Delta = \Gamma/10$ and (b) via SC proximity effect and with coupling to a pair of MBSs with $t = \Gamma/20$, $\Delta = \Gamma/20$, and $\epsilon_M = \Gamma/10$.

[1] V. Mourik, K. Zuo, S. M. Frolov, S. R. Plissard, E. P. A. M. Bakkers, and L. P. Kouwenhoven, Science **336**, 1003 (2012).

[2] J. R. Williams, A. J. Bestwick, P. Gallagher, S. S. Hong, Y. Cui, A. S. Bleich, J. G. Analytis, I. R. Fisher, and D. Goldhaber-Gordon, Phys. Rev. Lett. **109**, 056803 (2012).

[3] L. P. Rokhinson, X. Liu, and J. K. Furdyna, Nat. Phys. **8**, 795 (2012).
[4] M. T. Deng, C. L. Yu, G. Y. Huang, M. Larsson, P. Caroff, and H. Q. Xu, Nano Lett. **12**, 6414 (2012).
[5] A. Das, Y. Ronen, Y. Most, Y. Oreg, M. Heiblum, and H. Shtrikman, Nat. Phys. **8**, 887 (2012).
[6] C. W. J. Beenakker, Annu. Rev. Condens. Matter Phys. **4**, 113 (2013).
[7] J. Alicea, Rep. Prog. Phys. **75**, 076501 (2012).
[8] M. Leijnse and K. Flensberg, Semicond. Sci. Technol. **27**, 124003 (2012).
[9] A. Y. Kitaev, Ann. Phys. (Amsterdam) **303**, 2 (2003).
[10] J. Alicea, Y. Oreg, F. von Oppen, and M. P. A. Fisher, Nat. Phys. **7**, 412 (2011).
[11] S. Das Sarma, C. Nayak, and S. Tewari, Phys. Rev. B **73**, 220502(R) (2006).
[12] L. Fu and C. L. Kane, Phys. Rev. Lett. **100**, 096407 (2008).
[13] J. D. Sau, R. M. Lutchyn, S. Tewari, and S. Das Sarma, Phys. Rev. Lett. **104**, 040502 (2010).
[14] J. Alicea, Phys. Rev. B **81**, 125318 (2010).
[15] R. M. Lutchyn, J. D. Sau, and S. Das Sarma, Phys. Rev. Lett. **105**, 077001 (2010).
[16] Y. Oreg, G. Refael, and F. von Oppen, Phys. Rev. Lett. **105**, 177002 (2010).
[17] J. M. Byers and M. E. Flatté, Phys. Rev. Lett. **74**, 306 (1995).
[18] S. G. den Hartog, C. M. A. Kapteyn, B. J. van Wees, T. M. Klapwijk, and G. Borghs, Phys. Rev. Lett. **77**, 4954 (1996).
[19] Th. Martin, Phys. Lett. A **220**, 137 (1996).
[20] G. Lesovik, T. Martin, and G. Blatter, Eur. Phys. J. B **24**, 287 (2001).
[21] P. Recher, E. V. Sukhorukov, and D. Loss, Phys. Rev. B **63**, 165314 (2001).
[22] J. Rech, D. Chevallier, T. Jonckheere, and T. Martin, Phys. Rev. B **85**, 035419 (2012).
[23] K. T. Law, P. A. Lee, and T. K. Ng, Phys. Rev. Lett. **103**, 237001 (2009).
[24] C. J. Bolech and E. Demler, Phys. Rev. Lett. **98**, 237002 (2007).
[25] J. Nilsson, A. R. Akhmerov, and C. W. J. Beenakker, Phys. Rev. Lett. **101**, 120403 (2008).
[26] B. H. Wu and J. C. Cao, Phys. Rev. B **85**, 085415 (2012).
[27] A. Golub and B. Horovitz, Phys. Rev. B **83**, 153415 (2011).
[28] G. Strübi, W. Belzig, M.-S. Choi, and C. Bruder, Phys. Rev. Lett. **107**, 136403 (2011).
[29] S. B. Chung, X.-L. Qi, J. Maciejko, and S.-C. Zhang, Phys. Rev. B **83**, 100512(R) (2011).
[30] L. Hofstetter, S. Csonka, J. Nygård, and C. Schönenberger, Nature (London) **461**, 960 (2009).
[31] L. G. Herrmann, F. Portier, P. Roche, A. L. Yeyati, T. Kontos, and C. Strunk, Phys. Rev. Lett. **104**, 026801 (2010).
[32] A. Das, Y. Ronen, M. Heiblum, D. Mahalu, A. V. Kretinin, and H. Shtrikman, Nat. Commun. **3**, 1165 (2012).
[33] For the formation of "poor man's" Majorana states at zero energy, see M. Leijnse and K. Flensberg, Phys. Rev. B **86**, 134528 (2012).
[34] A. Y. Kitaev, Phys. Usp. **44**, 131 (2001).
[35] L. Fu, Phys. Rev. Lett. **104**, 056402 (2010).
[36] H.-F. Lü, H.-Z. Lu, and S.-Q. Shen, Phys. Rev. B **86**, 075318 (2012).
[37] See Supplemental Material at http://link.aps.org/supplemental/10.1103/PhysRevLett.111.036802 for additional information.
[38] Formally, we can decompose the QD fermion operators into a pair of Majorana operators each. There exists a particular decomposition for which only one of the dot Majoranas couples to the adjacent MBS. In the limit where one or both of the dot levels ϵ_L, $\epsilon_R = 0$, the two Majoranas in the dot are not coupled to each other, such that an uncoupled Majorana resides on the dot.
[39] M. P. Anantram and S. Datta, Phys. Rev. B **53**, 16390 (1996).
[40] B. Zocher, M. Horsdal, and B. Rosenow, Phys. Rev. Lett. **109**, 227001 (2012).
[41] S. Das Sarma, J. D. Sau, and T. D. Stanescu, Phys. Rev. B **86**, 220506(R) (2012).